Available online at www.sciencedirect.com
SCIENCE DIRECT®
International Journal of Heat and Mass Transfer 48 (2005) 3197–3211
International Journal of HEAT and MASS TRANSFER
www.elsevier.com/locate/ijhmt

Hydrodynamics and heat transfer in two-dimensional minichannels

Sylvain Reynaud [a], François Debray [b], Jean-Pierre Franc [a,*], Thierry Maitre [a]

[a] Laboratoire des Ecoulements Géophysiques et Industriels, CNRS-UJF-INPG, BP 53, 38041 Grenoble Cedex 9, France
[b] Laboratoire des Champs Magnétiques Intenses, CNRS-MPI, BP 166, 38042 Grenoble Cedex 9, France

Received 8 October 2004; received in revised form 10 December 2004
Available online 22 April 2005

Abstract

This work presents measurements of the friction and heat transfer coefficients in 2D minichannels of 1.12 mm to 300 μm in thickness. The friction factor is estimated from the measured pressure drop along the whole channel. The heat transfer coefficient is determined from a local and direct measurement of both temperature and heat flux at the wall using a specific transducer. The experimental results are in good agreement with classical correlations relative to channels of conventional size. The observed deviations are explained either by macroscopic effects (mainly entry and viscous dissipation effects) or by imperfections of the experimental apparatus.

1. Introduction

During the last two decades, most of the studies on heat transfer in microchannels highlighted heat transfer coefficients higher than those predicted on the basis of classical laws applicable to ducts of conventional size [1–3]. Other deviations with respect to traditional laws were also observed experimentally as unusual friction factors or shifts in the transition between laminar and turbulent regimes.

It is noteworthy that several studies exhibit contradictory results for both the mechanical and thermal characteristics of the flow. This is generally due to differences in the many parameters that characterize these studies such as the geometry (usually made of complex multichannels [4,5]), the hydraulic diameter, the shape and surface roughness of the channels, the fluid nature, the boundary conditions, the flow regimes and the measuring technique itself. Such a large variety of experimental conditions often makes difficult to apply the results of a given study to other experimental conditions. For a fundamental insight into microfluidics, it may then be useful to reduce as much as possible the number of parameters. This procedure was followed for example by Gao et al. [6] who chose a simple geometry and kept the same surface roughness whatever the channel thickness.

Two main categories of effects have been put forward to explain the deviations observed in microfluidics (see e.g. Tardu [7]): (i) macroeffects such as the effects of geometry or wall roughness and (ii) microeffects such as the effects of the electric double layer or gas rarefaction.

* Corresponding author. Tel.: +33 04 76 82 50 35; fax: +33 04 76 82 52 71.
E-mail address: jean-pierre.franc@hmg.inpg.fr (J.-P. Franc).

0017-9310/$ - see front matter © 2005 Elsevier Ltd. All rights reserved.
doi:10.1016/j.ijheatmasstransfer.2005.02.020

Nomenclature

C_f	friction factor $C_f = \frac{\tau}{\frac{1}{2}\rho V_b^2}$
D_H	hydraulic diameter (m)
e	minichannel thickness (m)
h	heat transfer coefficient (W m^{-2} K^{-1})
k_S	roughness (m)
l	minichannel width (m)
L	minichannel length (m)
L^+	non-dimensional minichannel length $L^+ = L/(D_H \times Re)^{-1}$
Nu	Nusselt number $Nu = \frac{hD_H}{\lambda}$
Po	Poiseuille number $Po = C_f \cdot Re$
Pr	Prandtl number
Q	volumetric flow rate (ℓ s^{-1})
Re	Reynolds number $Re = \frac{V_b D_H}{\nu}$
Re_x	Reynolds number based on the abscissa along the minichannel
T	temperature (°C)
V_b	channel bulk velocity (m s^{-1})
x	abscissa along the minichannel (m)
Z	aspect ratio $Z = l/e$

Greek symbols

δ_{99}	kinematic boundary layer thickness (m)
ΔP	pressure loss (bar)
φ	heat flux (W m^{-2})
λ	thermal conductivity (W m^{-1} K^{-1})
Λ	frictional resistance
μ	dynamic viscosity (kg m^{-1} s^{-1})
ν	kinematic viscosity (m^2 s^{-1})
ρ	density (kg m^{-3})
τ	wall shear stress (N m^{-2})

Subscripts

av	average (inlet/outlet)
aw	adiabatic wall (temperature)
in	inlet
out	outlet
w	minichannel wall

1.1. Macroeffects

Wu and Little [8] measured values of the friction factor higher than those expected (up to +60%) and a transition Reynolds number unexpectedly small (around 500). In the same way, Qu et al.[1] [9] observed, on the one hand, that the friction factor is up to 38% higher than that given by the theory and, on the other hand, that it increases when the hydraulic diameter decreases. The authors attributed this phenomenon to roughness. In a similar configuration[2] with smooth walls, Pfahler et al. [10] and then Flockhart et al. [11] obtained values of the friction factor in agreement with the theoretical predictions.

Wang and Peng [4,5] studied heat transfer for both laminar and turbulent regimes in a configuration close to that of Tuckerman and Pease [12] made up of several identical and parallel microchannels. Contrary to what the latter reported, Wang and Peng [4,5] observed that, in the laminar regime, the Nusselt number is lower than the theoretical one and exhibits a dependence with the Reynolds number. In the turbulent regime, they report that the Nusselt number is almost three times smaller than that given by the Colburn correlation (Eq. (5)) and that the transition Reynolds number (≅700) is lower than in the case of traditional ducts. These results contradict other studies such as Choi et al. [1] or Adams et al. [2] which conclude that the Nusselt number in the turbulent regime is higher than the expected values. Peng and Peterson [13] explain the discrepancies reported by Wang and Peng [4,5] by a reduction of the fluid viscosity along the channel due to a significant increase in temperature. The authors noticed that the Reynolds number could be doubled for an inlet value of about 1000. Although this effect of viscosity can explain a reduction in friction factor, it does not explain the increase of the Nusselt number with the Reynolds number in the laminar regime.

Zeighami et al. [14] obtained results similar to Wang and Peng. Their visualizations, in a microchannel of comparable geometry, show that transition to turbulence occurs for a Reynolds number around 1200–1600. With a similar experimental device,[3] Rahman [3] obtained very different results from those of Wang and Peng [4,5]. He indeed measured Nusselt numbers higher than those given by the classical correlations for both laminar and turbulent regimes. Moreover his results agree with the traditional values of both the friction factor in laminar conditions and the transition Reynolds number.

In a configuration close to the one used in the present work, Gao et al. [6] studied the hydrodynamics and heat

[1] $51 \leqslant D_H$ (μm) $\leqslant 169$, $100 \leqslant Re \leqslant 1500$.

[2] Isopropanol (779 kg/m^3), silicone oil (870 kg/m^3), $0.96 \leqslant D_H$ (μm) $\leqslant 40$, $5 \times 10^{-4} \leqslant Re \leqslant 70$.

[3] Twelve identical and parallel 1 mm wide channels with variable thickness ($300 \leqslant D_H$ (μm) $\leqslant 490$) are machined on a silicon plate ($600 \leqslant Re \leqslant 3000$).

transfer in a two-dimensional smooth channel.[4] They show that the friction factor follows the classical laws for both the laminar and turbulent regimes, whatever the hydraulic diameter. However, they report values of the Nusselt number lower than the theoretical ones for $D_H \leqslant 0.77$ mm and for both laminar and turbulent regimes, contrary to Rahman's results [3]. As for transition to turbulence, they report critical Reynolds numbers in agreement with classical values, contrary to the observations of Wang and Peng [4,5] and Zeighami et al. [14].

Some of the discrepancies mentioned above can be explained by entry effects. As an example, Pfahler et al. [10] report that the length required for developing the kinematic regime (which can reach 20% of the channel length in their configuration), can explain the raise in Poiseuille number with the Reynolds number in laminar conditions. These discrepancies can also be due to geometrical effects. In general, a channel with an aspect ratio $Z > 50$ can be regarded as two-dimensional with negligible edge effects. The rather low critical Reynolds numbers (around 700) found by Wang and Peng [4,5] (whose channels have an aspect ratio ranging between 1 and 4) could be caused by corner swirls [7].

Several authors highlighted the role played by wall roughness in the observed deviations [8,9]. According to Sabry [15], the wall shear stress, particularly high in microchannels, would give to the liquid flow a greater tendency to separate over the roughness elements. The flow would then be separated from the wall by a thin film of gas playing the role of a heat insulator. This could be a physical explanation when both the friction and heat transfer coefficients are below conventional values. But this model does not explain the raise of the friction factor with the roughness height pointed out by Wu and Little [8] and Acosta et al. [16]. The premature transition to turbulence and the raise of the Nusselt number with the Reynolds number in the laminar regime, observed by Wang and Peng [4,5], could be explained according to Sabry [15] by the presence of roughness elements locally higher than the average which would cause microswirls and likely enhance heat transfer. In the case of gases, the author indicates that a raise in the friction factor can be expected, which is not confirmed by other authors [1,10].

1.2. Microeffects

Mala et al. [17] were among the first to put forward the electric double layer (EDL) as a possible explanation of some experimental deviations observed in microfluidics. They showed that the EDL increases the wall shear stress and decreases heat transfer. However the dimensions of their microchannels are much smaller than those e.g. of Wang and Peng [4,5], and it can be expected that the EDL has actually a negligible influence on the results of most of the studies presented previously. This point is consolidated by the work of Ren et al. [18] who did not observe any significant effect of the EDL in the case of two-dimensional channels whose thickness is about 40 μm. Using Mala et al.'s theory, Tardu [7] shows that the EDL could also be the reason for a premature transition to turbulence. It is worth noticing that the size of the minichannels considered in the present work is much larger than those mentioned in this paragraph and, in particular, than those of Ren et al. [18]. The effect of the electric double layer can then be considered as negligible for this work.

In the case of gases, rarefaction effects can be expected for high enough values of the Knudsen number Kn. It is generally considered that the assumption of a continuous medium together with the no-slip condition at the wall are valid for $Kn < 10^{-3}$. On the contrary, for $Kn > 10$, the medium is highly rarefied and can no longer be regarded as continuous. For intermediate values of the Knudsen number (typically $10^{-3} \leqslant Kn \leqslant 10^{-1}$), the Navier–Stokes equations can still be used but the no-slip condition is no longer valid. The flow is then characterized by a slip velocity and a temperature jump at the boundaries. These wall discontinuities are major effects of rarefaction and could be responsible for some of the deviations observed in the case of gases. The numerical study of Tunc and Bayazitoglu [19] showed that the Nusselt number decreases when the Knudsen number increases and that this reduction is accentuated by a reduction of the aspect ratio (up to −70% for $Z = 10$).

2. Experimental apparatus and data processing

The experimental device was designed to investigate convective heat transfer in two-dimensional minichannels of height in the range 300 μm–1.12 mm. At the present time, our investigation is limited to single phase flow.

The test section is mounted in a hydrodynamic closed-loop (Fig. 1) which includes an upstream tank, a downstream tank (450 ℓ each) and a centrifugal pump (5.6 bar, 3.6 $\ell\,s^{-1}$). The tunnel is equipped with two electromagnetic flowmeters ($0.014\ \ell\,s^{-1} \rightarrow 2\ \ell\,s^{-1}$, ±0.5%), corresponding each to a different range in flowrate. The water temperature upstream and downstream of the test section is measured by means of Platinum probes (±0.05 °C). A differential pressure transducer gives the pressure drop along the whole channel ($0.2 \leqslant \Delta P(\text{bar}) \leqslant 20$, ± 0.012%). The fluid used is filtered tap water (mesh <5 μm).

[4] 200 μm $\leqslant D_H \leqslant$ 1.82 mm, $200 \leqslant Re \leqslant 8000$, the aspect ratio lies between 25 and 250.

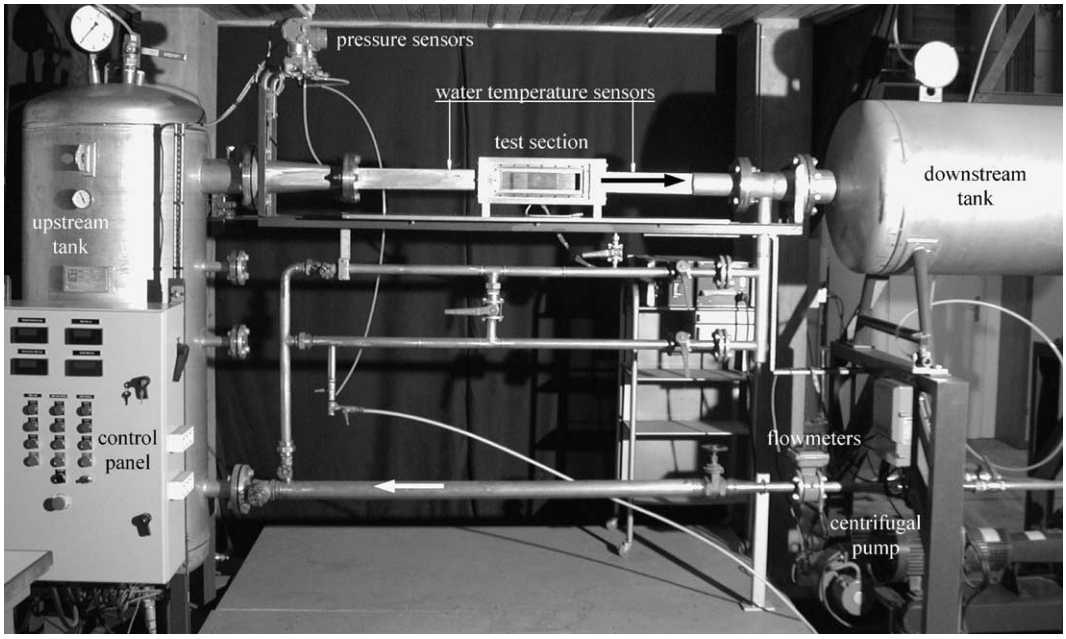

Fig. 1. Photograph of the hydrodynamic loop.

The test section is made of a bronze support ($370 \times 150 \times 80$ mm^3) in which a 60 mm wide and 20 mm thick flat channel was machined (Figs. 2 and 3). The channel walls were hand-polished and the average surface roughness measured by a Taylor–Hobson Surtronic 3+ system (accuracy $\cong 0.1$ μm) is $R_a \approx 0.25$ μm. The maximum height of the roughness elements was also measured; it is about 2 μm. This value is the mean value on ten data corresponding to the heights of the five highest peaks and the depths of the five deepest depressions with respect to the average line. The influence of roughness is discussed in Section 3.1. The test section was designed to receive on one side, interchangeable Plexiglas windows used to create the different minichannels in which the measurements are conducted and, on the other side, the heating block equipped with resistive cartridges intended to generate the surface heat flux (Figs. 2 and 3). It is worth noticing that the simple geometry of the test section gives to this study a rather fundamental character. It allows to easily insert a sensor for the direct measurement of both the heat flux and the wall temperature which is one of the originalities of this study. The design of the test section is such that the wall on which heat transfer is measured is unchanged and in particular its roughness is the same whatever the thickness of the channel.

The minichannels are 60 mm wide and 150 mm long (Figs. 2 and 3). Three windows are available leading to thickness of 1.12 mm, 540 μm and 300 m. These thicknesses have been measured using a TRIMESURE TEM-

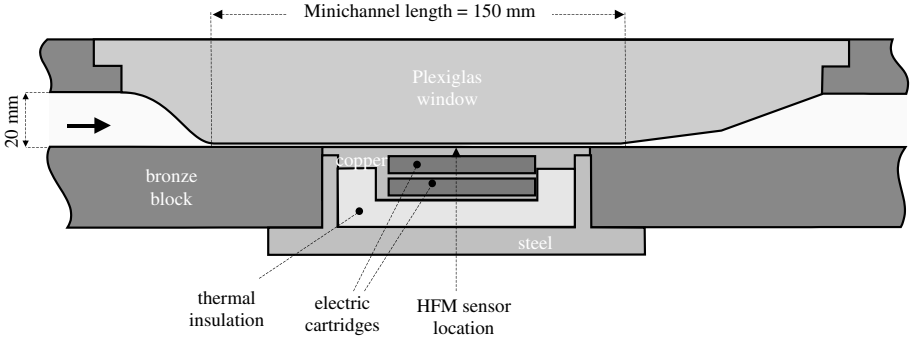

Fig. 2. Sketch of the test section (longitudinal view).

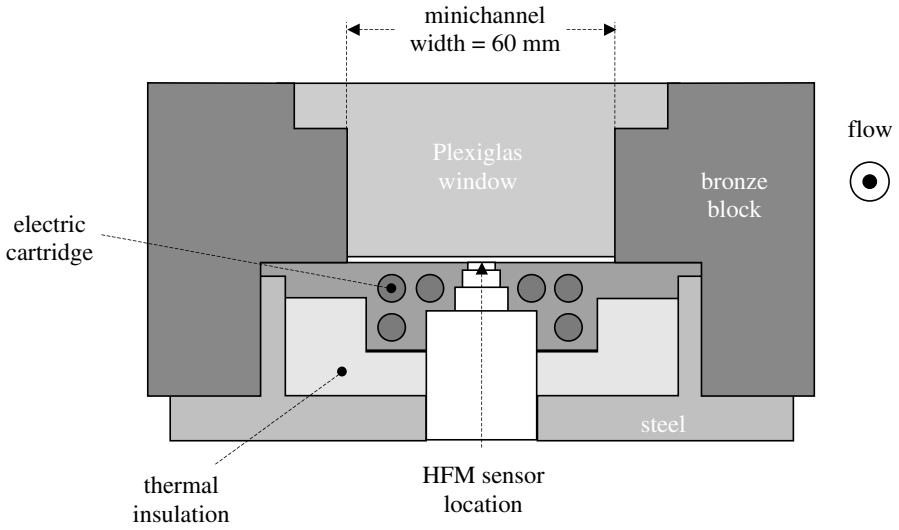

Fig. 3. Sketch of the test section (transversal view).

PO MCA7 robot controlled by the Metrolog software (±8 μm). Variations in thickness of 35 μm on an average over the width of the minichannels were measured. They are due to the deformation of the Plexiglas window, probably caused by hand-polishing and the successive assemblies of the windows on the bronze block. The three thicknesses indicated above take into account these irregularities and correspond to mean values. The minichannels can be regarded as two-dimensional since the aspect ratio lies between 54 and 200. The windows, more especially the convergent and the divergent, were designed to minimize the singular pressure losses at the inlet and outlet. The length of the channels is the result of a compromise between the length necessary for the kinematic regime to develop and our objective to investigate flows of relatively high velocity. A long channel actually induces high pressure losses and then a drop in the flow rate. Table 1 summarizes the mean velocity and Reynolds number ranges which can be investigated for each channel. The maximum flow velocity is 24 m s^{-1} for the channel of 1.12 mm in thickness. It drops to 13 m s^{-1} for the smaller one (300 μm).

The heating block is mounted on the lower side of the bronze support (Figs. 2 and 3). It is the only hot wall of the minichannel. It is made out of copper and thermally insulated on its outside part. It contains six resistive cartridges of 6.5 mm in diameter and 55 mm in length supplied with an electric power of about 900 W. The resulting measured heat flux is of the order of 10 W/cm^2. The heating block is also equipped with a flush mounted HFM-7 E/L sensor developed by Vatell Corporation (Fig. 4) which allows a direct and local measurement of both the heat flux (±0.1%) and the wall temperature (±0.5%). The sensor is located at 90 mm from the inlet of the minichannel and at 25 mm from the inlet of the heated zone (Fig. 2). The kinematic regime is fully developed or almost fully developed at the sensor location for both laminar and turbulent regimes (see Section 3.1 for more details). As for the thermal regime, it cannot be considered as fully developed at the location of the sensor because of the relatively short length of the heated zone [20]. It is noteworthy that the short rise time of the HFM sensor (about 6 μs) allowed observations of the instantaneous fluctuations of the heat flux and the wall temperature when transition to turbulence occurs (see Section 3.2).

Table 1
Channel bulk velocity ranges and Reynolds number ranges

Channel thickness	Channel bulk velocity range	Reynolds number range
1.12 mm	$0.9 \leqslant V_b$ (m s^{-1}) $\leqslant 24$	$2500 \leqslant Re \leqslant 72{,}000$
540 μm	$0.8 \leqslant V_b$ (m s^{-1}) $\leqslant 18$	$1400 \leqslant Re \leqslant 25{,}000$
300 μm	$0.7 \leqslant V_b$ (m s^{-1}) $\leqslant 13$	$600 \leqslant Re \leqslant 10{,}000$

The data are presented in terms of variations of the Poiseuille and Nusselt numbers with the Reynolds number. All of them are based on the hydraulic diameter D_H which is close to 2e in our case of a nearly two-dimensional channel. The water properties are estimated at the average temperature T_{av} between inlet and outlet. The theoretical determination of the measurement uncertainties should take into account the thermal expansion of the Plexiglas windows. It is difficult to estimate this effect satisfactorily since we cannot measure the channel thickness during the experiments, nor even determine the temperature field in the window. In our configuration, thermal expansion tends to reduce the

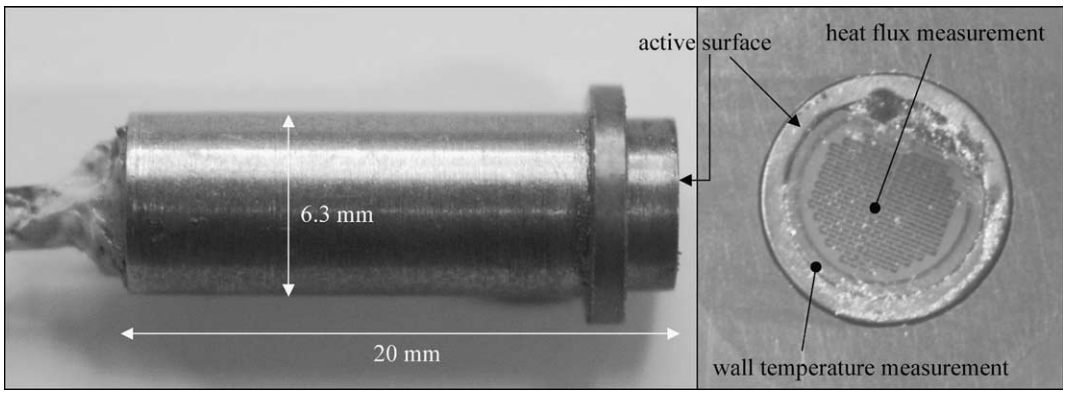

Fig. 4. Heat flux microsensor.

channel thickness. For a rough estimate, we assumed that the window temperature is uniform and equal to the maximum water temperature. This gives an upper limit to the reduction in channel thickness of about 20 μm for the most critical case. Hence, the uncertainty on the channel thickness due to thermal expansion is comparable to that due to machining previously estimated at 35 μm. The uncertainties given in Table 2 do not take into account thermal expansion because of the difficulty to estimate it properly. They are based on the maximum differences observed during measurements (on about twenty couples of points) and then give an estimate of the measurement reproducibility defect.

Measurements are taken in steady state, i.e. when all the measured values ($Q, \Delta P, T_{\text{in}}, T_{\text{out}}, T_{\text{w}}, \varphi$) are stable on an average. Hydrodynamic and heat transfer measurements are generally conducted simultaneously.

In order to support the interpretation of the experimental results, a numerical computation of the flow in the minichannels has been made using the Fluent code. The main objective is to provide information which cannot be obtained through experiments because of an instrumentation in heat flux and wall temperature limited to a unique location. In particular, it allowed us to estimate entry effects which could not be investigated experimentally.

Our measurements will be compared to classical results in the laminar and turbulent regimes. For the laminar regime, it can be shown analytically that, in the case of a fully developed flow, the Poiseuille number is constant

$$Po = 24 \tag{1}$$

In the case of the flow between two infinite flat plates with a constant heat flux on one side and an adiabatic condition on the opposite one, the Nusselt number is also constant

$$Nu \cong 5.385 \tag{2}$$

For the fully developed turbulent regime ($4000 < Re < 10^5$) and in the case of smooth walls, the Poiseuille number can be approximated by the following empirical relation:

$$Po = 0.079 Re^{0.75} \tag{3}$$

The transition from hydraulically smooth to completely rough flows can be described by Colebrook's equation which gives the frictional resistance Λ as a function of the Reynolds number and the relative roughness k_S/D_{H}

$$\frac{1}{\sqrt{\Lambda}} = -2\log\left[\frac{2.51}{Re\sqrt{\Lambda}} + \frac{k_S}{3.71 D_{\text{H}}}\right] \tag{4}$$

For the Nusselt number, we use as a reference the classical Colburn correlation [21] which proved to be adequate for the interpretation of the present experimental results

$$Nu = 0.023 Re^{0.8} Pr^{1/3} \tag{5}$$

As mentioned previously, the pressure drop is measured between two stations of the inlet and outlet pipes, one being located upstream the convergent and the other one downstream the divergent (these stations are denoted u and d in Fig. 5). Then, this estimate of the pressure drop includes pressure drops in the divergent and in the convergent. In order to estimate the influence of the measuring procedure, a few additional measurements were conducted between two stations located inside the minichannel itself and separated with a distance of

Table 2
Measurement reproducibility: maximal deviation observed for *Po* and *Nu* numbers between the different series of measurements at a given Reynolds number and for a given channel

	$e = 1.12$ mm	$e = 540$ μm	$e = 300$ μm
$\frac{\Delta Po}{Po}$	5%	3%	13%
$\frac{\Delta Nu}{Nu}$	12%	14%	12%

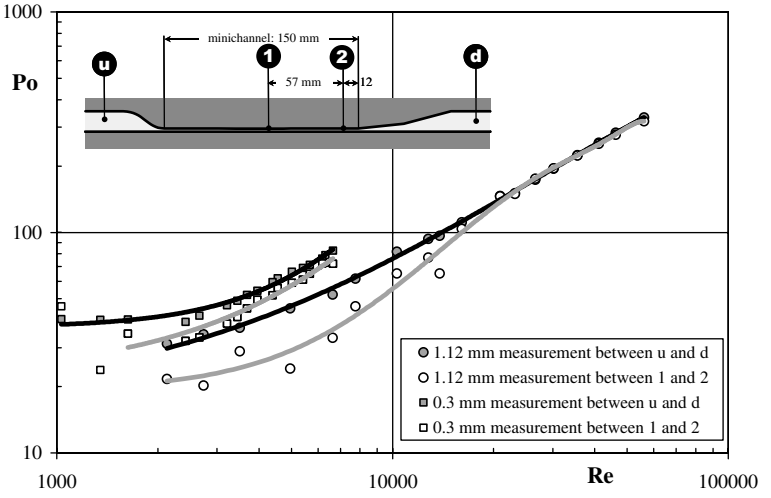

Fig. 5. Influence of the location of the measuring stations on the Poiseuille number.

57 mm (stations 1 and 2 in Fig. 5). The pressure holes are 0.2 mm in diameter. Only a limited number of measurements were made for the largest and the smallest channel. The results are presented in Fig. 5. It appears that the two sets of measurements are in reasonable agreement, especially at high Reynolds number. The friction factor estimated from the pressure drop along the whole test section can then be considered as representative of the friction factor inside the minichannel, especially for the turbulent regime.

3. Results and discussion

3.1. Hydrodynamics

For $Re < 4000$, Fig. 6 shows that, in the case of the thickest channel ($e = 1.12$ mm), the Poiseuille number is somewhat larger than the value predicted by Eq. (1) and in addition, it slightly increases with the Reynolds number. These deviations are due to entry effects since the measurements are in quite good agreement with the equation derived by Shah and London [22] for laminar flows in two-dimensional channels which corrects the Poiseuille number according to the non-dimensional length L^+ of the minichannel

$$Po = \frac{3.44}{\sqrt{L^+}} + \frac{24 + \frac{0.674}{4L^+} - \frac{3.44}{\sqrt{L^+}}}{1 + \frac{2.9\times10^{-5}}{L^{+2}}} \tag{6}$$

The numerical simulations confirm this conclusion and show that the length necessary for the development of the kinematic regime represents 60% of the minichannel length for $Re \cong 3000$, so that entry effects actually appear to be non-negligible.

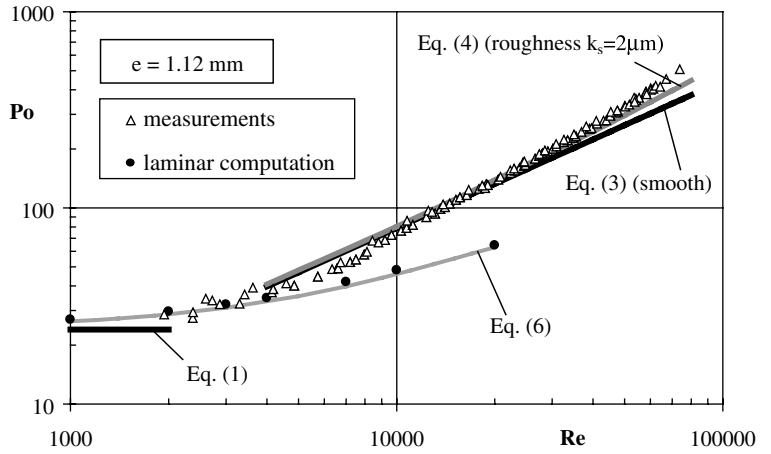

Fig. 6. Variations of the Poiseuille number with the Reynolds number ($e = 1.12$ mm).

For the turbulent regime, at large Reynolds number, the values of the Poiseuille number are compared to the values given by (i) Eq. (3) relative to the smooth turbulent regime and (ii) the Colebrook's equation (4) in which k_S has been set to 2 μm according to the roughness measurements. The evolution of the Poiseuille number with the Reynolds number is more correctly described by Colebrook's correlation taking into account a roughness effect than by a $Re^{3/4}$ law which characterizes the hydraulically smooth regime. Then, the present measurements point out a non-negligible roughness effect for a relative roughness of about $k_S/D_H = 0.09\%$. Acosta et al. [16] observed a similar behaviour in a rectangular channel ($D_H = 953$ μm) with a relative roughness $k_S/D_H = 0.2\%$. They report that the friction factor follows the smooth regime only for very small values of the relative roughness, smaller than typically 0.005%.

The same conclusions apply to the case of the minichannel of middle thickness ($e = 540$ μm) for both the laminar and turbulent regimes (Fig. 7). However, for $Re < 700$, the Poiseuille number is slightly smaller than the theoretical value given by Eq. (1) (−17% for $Re \cong 300$). Pfahler et al. [23] reported similar observations and imputed this phenomenon to variations in the physical properties of the fluid due to temperature effects. In our case, it has been observed that free convection effects arise for such low flow rates. This is confirmed by estimates of the order of magnitude of the Richardson number (the ratio of the Grashof to the Reynolds number squared) which is typically of the order of 14. Free convection effects are then expected [15] and the water temperature is no longer uniform throughout the outlet cross-section so that the measurement in the middle of this section is no longer relevant of the liquid bulk temperature.

In the case of the channel of smallest thickness (300 μm), Fig. 8 shows a relatively more important scatter of the measuring points which does not allow the detection of any influence of entry effects as done previously. It can be considered then that the laminar Poiseuille number is almost independent of the Reynolds number, as predicted by the theory. The average value of the Poiseuille number (≅38) is about 60% larger than that given by Eq. (1). In a configuration close to ours and in the case of a channel of same thickness, Gao et al. [6] did not observe such a difference and reported values of the Poiseuille number in agreement with the theory. It should however be noticed that their walls have a smaller relative roughness ($k_S/D_H < 0.06\%$) in comparison with the present case for which the relative roughness is about 0.3%. Values of the Poiseuille number larger than the theoretical ones might then be due to a roughness effect. This phenomenon was already pointed out by Qu et al. [9] who observed and checked numerically that the friction factor can be from 8% to 38% higher than the theory in the case of a relative roughness of about 2%. They indicate that surface roughness might enhance momentum transfer in the boundary layer, resulting in an increase of the friction factor. This phenomenon can be accounted for by introducing a roughness viscosity which is similar to the usual eddy viscosity in turbulent flows. In a recent study, Bavière et al. [24] confirmed that roughness considerably increases the friction coefficient in the laminar regime. Their analysis shows that a rough channel is actually equivalent to a smooth one provided its thickness is reduced by a value of the order of twice the height of the roughness elements. This tends to prove that the small scale recirculations which develop behind the roughness elements generate dead layers along each of the two channel walls and then reduces the effective cross-sectional area of the microchannel.

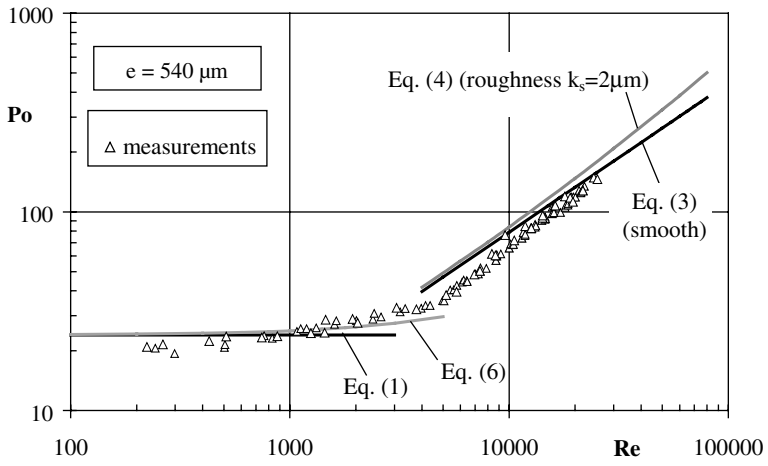

Fig. 7. Variations of the Poiseuille number with the Reynolds number ($e = 540$ μm).

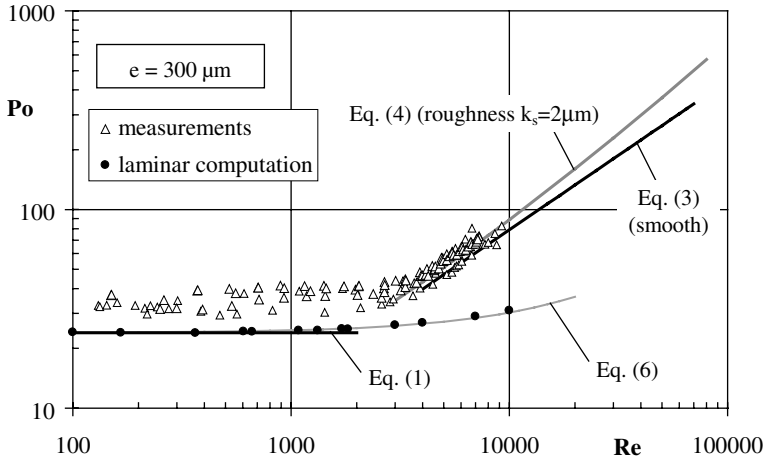

Fig. 8. Variations of the Poiseuille number with the Reynolds number (e = 300 µm).

For the turbulent regime (i.e. for $Re > 4000$), the variations of the Poiseuille number with the Reynolds number are in agreement with Colebrook's equation using the same value for the roughness k_S = 2 µm.

A comparison of the evolution of the Poiseuille number with the Reynolds number is given in Fig. 9 for the three minichannels. The measurements corresponding to the two thickest channels are relatively close to each other. When comparing these two sets of data, there is a slight tendency for the Poiseuille number to decrease when the hydraulic diameter decreases as reported by Pfahler et al. [10]. However, this tendency is not confirmed by the measurements corresponding to the smallest channel which are definitely higher than the two preceding ones. Thus the present investigation does not enable us to identify a clear effect of the size of the minichannel on wall friction. The higher values of the Poiseuille number for the smallest channel were attributed to a roughness effect and an increased relative roughness k_S/D_H when the hydraulic diameter decreases since the absolute roughness is unchanged for all the experiments.

In addition, the evolution of the Poiseuille number with the Reynolds number shows that transition to turbulence (more clearly visible in the two cases e = 540 µm and 300 µm) in such minichannels occurs for Reynolds numbers ranging between 3000 and 5000. This critical value is in general agreement with the usual critical Reynolds number in channels of conventional size.

3.2. Heat transfer

The evolution of the Nusselt number with the Reynolds number is plotted on Fig. 10 for the channel of

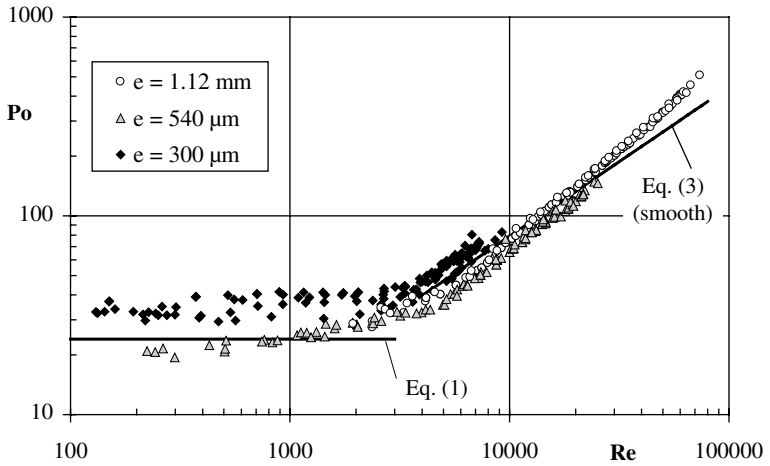

Fig. 9. Variations of the Poiseuille number with the Reynolds number. Comparison between the three thicknesses.

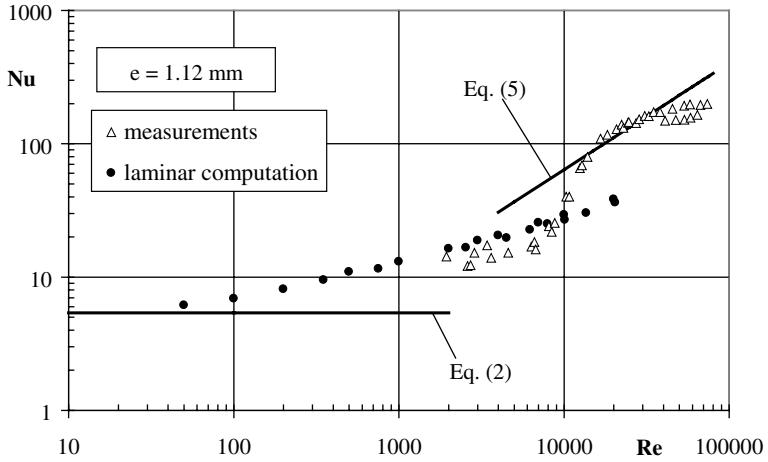

Fig. 10. Variations of the Nusselt number with the Reynolds number ($e = 1.12$ mm).

1.12 mm in thickness. Three zones can be identified. The first one corresponds to the laminar regime and extends up to $Re \cong 7000$. In this zone, the Nusselt number is somewhat higher than the value given by Eq. (2) and increases with the Reynolds number. Rahman [3] made similar observations and attributed this phenomenon to the development of the thermal boundary layers. This assumption is corroborated by our computation of the laminar flow. The corresponding numerical results are also given on Fig. 10. They prove that the thermal regime is not fully developed at the location of the sensor for $Re > 50$.

For intermediate values of the Reynolds number (typically $7000 < Re < 16{,}000$), instantaneous fluctuations of high amplitude for both the wall temperature and the heat flux were observed during the tests (Fig. 11b). This zone corresponds to transition to turbulence and more precisely to a transitional boundary layer characterized by the intermittent development of turbulent spots which are convected downstream and which induce large fluctuations of the heat flux and the wall temperature as they pass over the sensor. These observations are made possible by the short rise time of the HFM sensor of the order of 6 μs, which is much smaller than the transit time of a fluid particle over the characteristic diameter of the sensor which lies between 1.1 ms and 2.5 ms in the range of flowrate corresponding to this zone.

The transition zone corresponds to critical values of the Reynolds number higher than those pointed out by the evolution of the Poiseuille number with the Reynolds number (cf. Fig. 9). This is due to the fact that the Poiseuille number is here estimated from the measurement of the pressure drop along the whole channel and then represents a global measurement whereas the Nusselt number represents a local one.

Table 3 summarizes the Reynolds number ranges, based on the hydraulic diameter, in which high fluctuations of the heat transfer coefficient were observed, for the three different minichannels. We also indicate the Reynolds number Re_x based on the distance $x = 90$ mm from the HFM sensor to the minichannel inlet. The corresponding values are characteristic of the critical Reynolds number Re_x for a boundary layer flow on a flat plate which usually lies between 3×10^5 and 10^6 [25]. As a reference, the typical thickness δ_{99} of the laminar boundary layer at 99% [25]

$$\delta_{99} \cong \frac{5x}{\sqrt{Re_x}} \tag{7}$$

is also indicated. If it is clear that the laminar boundary layers on the two opposite walls actually fill the entire channel at the HFM sensor location in the case of the smallest channel and then that the flow can be considered as fully developed, this is not the case for the thickest one ($e = 1.12$ mm). Our numerical study confirmed these conclusions.

Moreover, the transition from laminar to turbulent is more gradual for the Poiseuille number than for the Nusselt number. Actually, as the Reynolds number increases, transition to turbulence moves progressively upstream. When it passes over the transducer, the flow switches rather suddenly from laminar to turbulent and the change in Nusselt number is then relatively marked. In contrast, the change in Poiseuille number is much more gradual since turbulence gradually spreads to the minichannel. Fully turbulent flow is obtained only when transition has reached the upstream part of the channel. The transition observed on the pressure drop is then smoother.

For high values of the Reynolds number ($Re > 16{,}000$ in the case $e = 1.12$ mm), the regime is fully

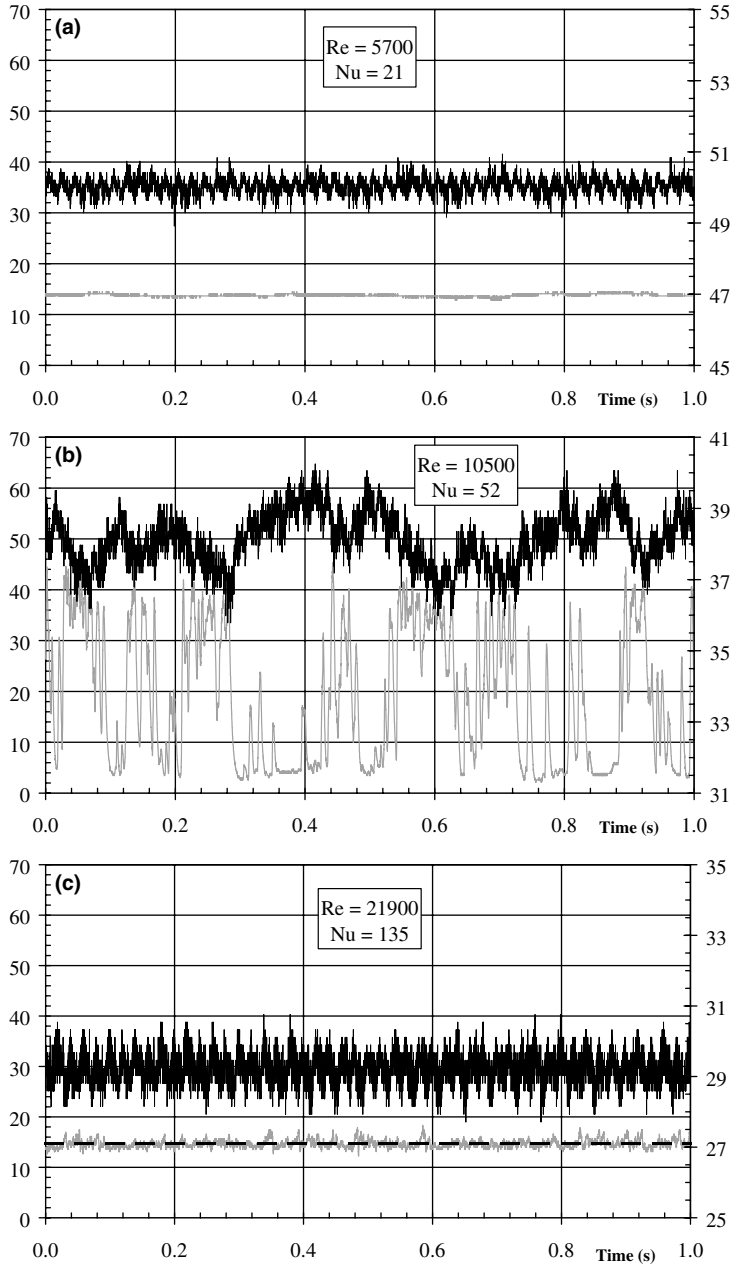

Fig. 11. Signals corresponding to the heat flux (grey, left hand-side scale, W/cm^2) and the wall temperature (black, right hand-side scale, °C) as functions of time for different Reynolds numbers (e = 1.12 mm).

Table 3
Transition Reynolds numbers for the three minichannels

Channel thickness (μm)	Transition Reynolds number based on the hydraulic diameter	Transition Reynolds number Re_x (based on x = 90 mm)	Laminar boundary layer thickness δ_{99} (μm)
300	3000–4500	4.5×10^5–6.8×10^5	550–670
540	7000–13,000	5.8×10^5–1.1×10^6	430–590
1120	7000–16,000	2.8×10^5–6.4×10^5	560–850

turbulent (Fig. 10). The large fluctuations observed in the transition zone clearly decrease and get stabilized at a RMS value which is however larger than for the laminar regime (Fig. 11c). The values of the Nusselt number are close to those given by Eq. (5) and actually follow a $Re^{0.8}$ power law. However for $Re > 30{,}000$, the Nusselt number deviates from the Colburn's correlation (5). This deviation is due to two main effects, viscous dissipation and a lack of uniformity of the heat flux.

Viscous dissipation is an additional source of heat which is no longer negligible at the highest flow velocities. Recent works (such as [26,27]) have shown that, for microchannels, the contribution of viscous dissipation to the energy balance may become significant because of the large velocity gradient in the boundary layers. When dissipation is considered, it is generally assumed that the same heat transfer correlations are valid provided the heat transfer coefficient is computed using the difference between the actual wall temperature T_w and the adiabatic wall temperature T_{aw} instead of the bulk temperature T_{av} [28]. In order to estimate the viscous dissipation, the difference $\Delta T_{\varphi=0}$ between the wall temperature and the bulk temperature T_{av} was systematically measured in the adiabatic case (i.e. with zero heat flux) as a function of the Reynolds number. In the case of a non-zero heat flux, the adiabatic wall temperature is approximated by $T_{aw} = T_{av} + \Delta T_{\varphi=0}$ and the Nusselt number by

$$Nu = \frac{D_H \varphi}{\lambda(T_w - T_{av} - \Delta T_{\varphi=0})} \tag{8}$$

The correction for viscous dissipation represented by the term $\Delta T_{\varphi=0}$ in the previous equation leads to slightly higher values of the Nusselt number since the temperature difference is slightly smaller in Eq. (8). Fig. 12 presents a comparison between the original and corrected values of the Nusselt number. For this thick channel, the correction appears non-negligible for Reynolds numbers larger than about 40,000 although it only partly explains the deviation. This point is more especially true in the case of the two other thinner minichannels since maximum flow velocities are smaller, inducing smaller viscous dissipation.

In addition to viscous dissipation, the lack of uniformity of the heat flux is another phenomenon which leads to underestimate the Nusselt number at high velocities. Despite the cares which were taken for mounting the sensor, it is likely that the surface heat flux drops at the location of the sensor because of a locally higher thermal resistivity. At high velocities, the transit time is so small that the wall temperature has not enough time to continuously adjust to the drop of heat flux. At the sensor location, the wall temperature is then higher than that which would correspond to a uniform heat flux equal to the flux at the sensor location. The Nusselt number is then underestimated. Although it is difficult to quantify this effect, computations of the thermal boundary layer taking into account an estimated non-uniform distribution of the surface heat flux qualitatively confirmed this trend. In conclusion, the deviation observed at high Reynolds number on Fig. 10 is most likely due to the combined effects of viscous dissipation and a lack of uniformity of the heat flux.

The variations of the Nusselt number with the Reynolds number for the two other minichannels are given in Figs. 13 and 14. They show the same behaviour as for the thickest one and the comments made in the case $e = 1.12$ mm are still valid for the two smaller channels. A specific feature is noticed in the case $e = 300\ \mu m$ (Fig. 14) for which the Nusselt number is lower than

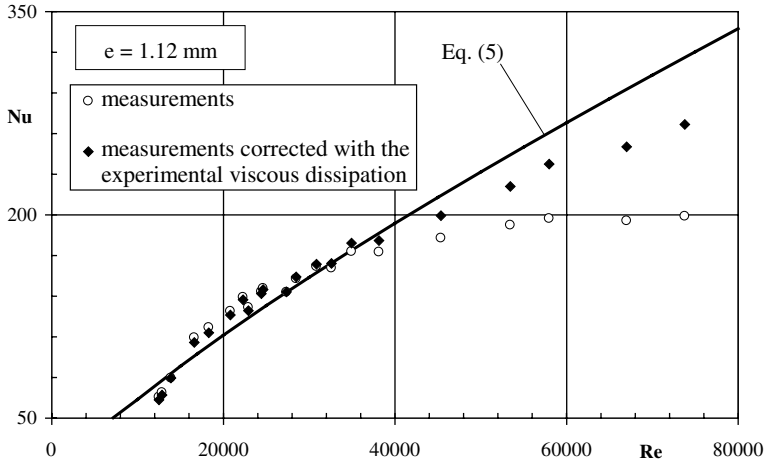

Fig. 12. Variations of the Nusselt number with the Reynolds number ($e = 1.12$ mm). Comparison between the original and corrected (with the experimental viscous dissipation) values of the Nusselt number.

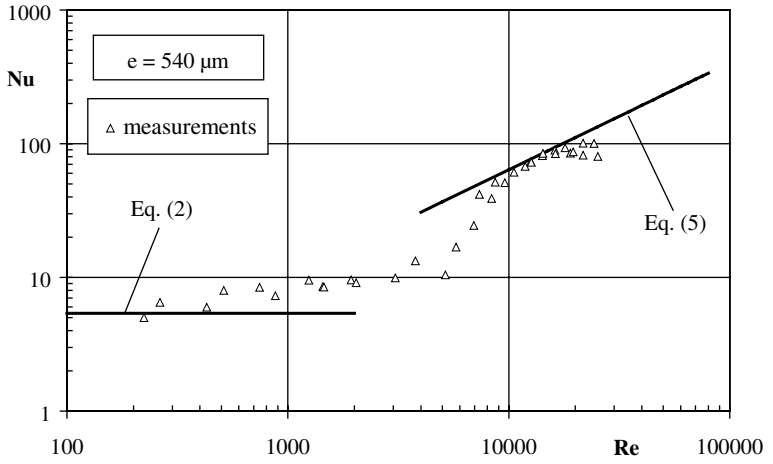

Fig. 13. Variations of the Nusselt number with the Reynolds number (e = 540 μm).

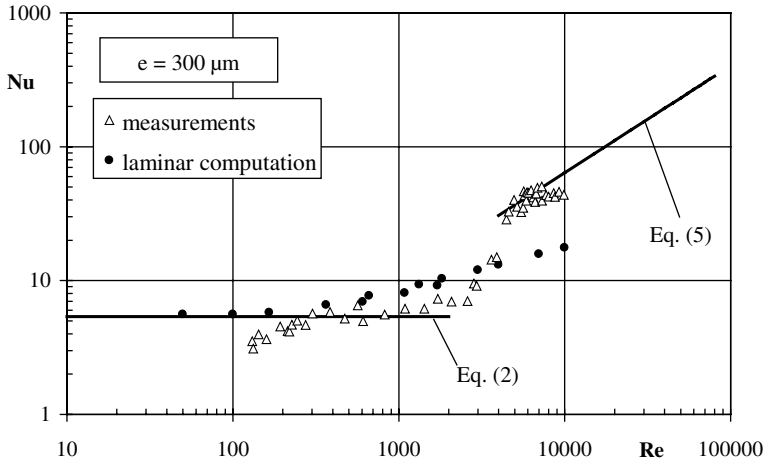

Fig. 14. Variations of the Nusselt number with the Reynolds number (e = 300 μm).

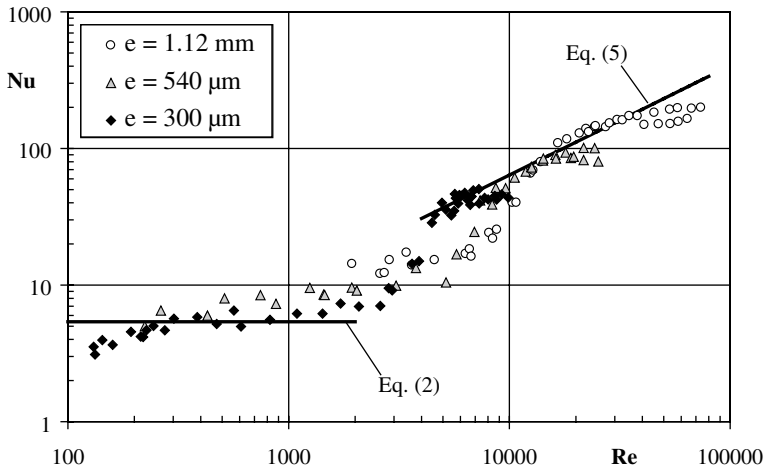

Fig. 15. Variations of the Nusselt number with the Reynolds number. Comparison between the three thicknesses.

the value given by Eq. (2) for very small Reynolds numbers (typically $Re < 300$). This difference, which increases when the Reynolds number decreases, is assigned to free convection effects downstream of the minichannel which are no longer negligible at relatively low flowrates, as already mentioned in Section 3.1.

Fig. 15 presents a comparison of our experimental data on heat transfer for the three channels. In the laminar regime, they are relatively close to each other and follow the same trend with the Reynolds number. For the turbulent regime, if we ignore the decrease in Nusselt number which is observed for all three channels at high flow rate and which is partly due to an imperfection of the heating device, it appears that the values of the Nusselt number are close to those given by the classical Colburn correlation.

4. Conclusion

Hydrodynamics and heat transfer have been investigated in two-dimensional minichannels of 1.12 mm, 540 μm and 300 μm in thickness. One wall is heated with a maximum heat flux of about 10 W/cm^2, whereas the opposite one is adiabatic. The present investigation is limited to single phase flow. Both the laminar and the turbulent regimes were investigated with a maximum flow velocity of 24 m s^{-1}, 18 m s^{-1} and 13 m s^{-1} respectively. From a hydrodynamic viewpoint, the friction factor was determined from the measurement of the pressure drop along the whole channel. As for the convective heat transfer coefficient, it was determined from a simultaneous and local measurement of both the temperature and the heat flux on the wall using a specific sensor. The results are presented in terms of the variation of the Poiseuille and the Nusselt numbers as a function of the Reynolds number. The measurement reproducibility is characterized by a maximal scattering of the Poiseuille and Nusselt numbers equal to 14%.

The main conclusions of this work are the following.

1. In the laminar regime and for the two thickest channels, the measured Poiseuille number is close to the theoretical value $Po = 24$. It slightly increases with the Reynolds number because of entry effects. For the 300 μm channel, although the scattering of the experimental data is more important, the Poiseuille number is larger on an average and its mean value is about 38. This deviation might be due to roughness effects as observed by other investigators [9,24].
2. In the turbulent regime and for the three minichannels, the values of the Poiseuille number are in general agreement with the usual correlations and more especially with Colebrook's correlation taking into account a roughness effect. At constant Reynolds number, the experimental data exhibit a slight decrease of the Poiseuille number between the case 1.12 mm and 540 μm. The trend is opposite between 540 μm and 300 μm, so that no definite effect of the size of the minichannel on wall friction can be drawn from the present investigation.
3. The evolution of the Poiseuille number with the Reynolds number shows that transition to turbulence occurs for Reynolds number between 3000 and 5000. This range is in agreement with the usual values of the critical Reynolds number relative to channels of conventional size.
4. In the laminar regime, the Nusselt numbers for the three minichannels are very close. The values are a little higher than the steady-state value and shows a slight increase with the Reynolds number. This proves that the thermal regime is not fully developed at the sensor location. For the minichannel of 300 μm in thickness, measurements of the Nusselt number at very low flowrates are altered by free convection effects.
5. In the turbulent regime, the evolution of the Nusselt number with the Reynolds number is in quite good agreement with Colburn's correlation. A deviation is observed for all three minichannels at high Reynolds number. It is due to viscous dissipation and also to a lack of uniformity of the heat flux along the wall.
6. Between the laminar and the turbulent regimes, a transition regime could be identified for the thermal boundary layer. It is characterized by high fluctuations of both the local wall temperature and the heat flux which are the signature of the transit of turbulent bursts over the transducer. Such an observation was possible because of the very short rise time of the transducer. The domain of transition is in agreement with the usual values of the critical Reynolds number for a boundary layer flow.

In conclusion, the present work does not exhibit significant deviations for the evolutions of both the Poiseuille number and the Nusselt number with the Reynolds number in comparison with the classical laws widely used for the prediction of heat transfer in larger channels. This conclusion, obtained for two-dimensional channels of minimum thickness 300 μm, is in agreement with other recent studies (e.g. [29]) which indicate that there is no difference between micro and macro flows provided secondary phenomena such as roughness, EDL, compressibility... remain of minor influence. The deviations which were observed here could be explained by macroeffects (mainly entry effects, viscous dissipation, free convection) or by imperfections of our experimental device especially for convective heat transfer measurements at high velocity. Hence, our experimental data and associated accuracy tend to prove

that, if an effect of the channel size actually exists, it will cause only a weak departure from the classical laws in the present domain of investigation.

Acknowledgement

The authors are grateful to Michel Riondet for his technical assistance during experiments and to Thibaud Renou for additional measurements.

References

[1] S.B. Choi, R.F. Barron, R.O. Warrington, Fluid flow and heat transfer in microtubes, Micromech. Sensors Actuators Syst. 32 (1991) 123–134.
[2] T.M. Adams, S.I. Abdel-Khalik, S.M. Jeter, Z.H. Qureshi, An experimental investigation of single-phase forced convection in microchannels, Int. J. Heat Mass Transfer 41 (6–7) (1997) 851–857.
[3] M.M. Rahman, Measurements of heat transfer in microchannel heat sinks, Int. Commun. Heat Mass Transfer 27 (4) (2000) 495–506.
[4] B.X. Wang, X.F. Peng, Experimental investigation on liquid forced convection heat transfer through microchannels, Int. J. Heat Mass Transfer 37 (Suppl. 1) (1994) 73–82.
[5] X.F. Peng, B.X. Wang, G.P. Peterson, H.B. Ma, Experimental investigation of heat transfer in flat plates with rectangular microchannels, Int. J. Heat Mass Transfer 38 (1) (1995) 127–137.
[6] P. Gao, S. Le Person, M. Favre-Marinet, Scale effects on hydrodynamics and heat transfer in two-dimensional mini and microchannels, Int. J. Thermal Sci. 41 (2002) 1017–1027.
[7] S. Tardu, Transferts thermiques dans les micro-canaux, Microfluidique, Traité EGEM, Tome 6 Chapitre 6, Hermès, 2002.
[8] P. Wu, W.A. Little, Measurement of friction factors for the flow of gases in very fine channels used for microminiature Joule-Thomson refrigerators, Cryogenics 23 (5) (1983) 273–277.
[9] W. Qu, Gh.M. Mala, D. Li, Pressure-driven water flows in trapezoidal silicon microchannels, Int. J. Heat Mass Transfer 43 (3) (2000) 353–364.
[10] J. Pfahler, J. Harley, H.H. Bau, J.N. Zemel, Gas and liquid flow in small channels, Micromech. Sensors Actuators Syst. 32 (1991) 49–60.
[11] S.M. Flockhart, R.S. Dhariwal, Experimental and numerical investigation into the flow characteristics of channels etched in ⟨100⟩ Silicon, J. Fluid Eng. 120 (1998) 291–295.
[12] D.B. Tuckerman, R.W.F. Pease, High-performance heat sinking for VSLI, IEEE Electron Dev. Lett. EDL-2 (5) (1981) 126–129.
[13] X.F. Peng, G.P. Peterson, The effect of thermofluid and geometrical parameters on convection of liquids through rectangular microchannels, Int. J. Heat Mass Transfer 38 (4) (1995) 755–758.
[14] R. Zeighami, D. Laser, P. Zhou, M. Asheghi, S. Devasenathipathy, T. Kenny, J. Santiago, K. Goodson, Experimental investigation of flow transition in microchannels using micron-resolution particle image velocimetry, in: Proceedings of IEEE ITHERM 2000: The Seventh Intersociety Conference on Thermal and Thermomechanical Phenomena in Electronic Systems, vol. 2, 2000, pp. 148–153.
[15] M.N. Sabry, Scale effects on fluid flow and heat transfer in microchannels, in: Proceedings of Conference Therminice, Rome, 1999, pp. 193–198.
[16] R.E. Acosta, R.H. Muller, C.W. Tobias, Transport process in narrow (capillary) channels, AIChE J. 31 (3) (1985) 473–482.
[17] G.M. Mala, D. Li, J.D. Dale, Heat transfer and fluid flow in microchannels, Int. J. Heat Mass Transfer 40 (13) (1997) 3079–3088.
[18] L. Ren, W. Qu, D. Li, Interfacial electrokinetic effects on liquid flow in micro-channels, Int. J. Heat Mass Transfer 44 (2001) 3125–3134.
[19] G. Tunc, Y. Bayazitoglu, Heat transfer in rectangular microchannels, Int. J. Heat Mass Transfer 45 (4) (2002) 765–773.
[20] S. Reynaud, Transferts thermiques par convection forcée en mini-canaux, Ph.D. thesis, Institut National Polytechnique de Grenoble, France, 2003.
[21] W.M. Rohsenow, J.P. Hartnett, Handbook of Heat Transfer, McGraw-Hill, New York, 1973.
[22] R.K. Shah, A.L. London, Laminar flow forced convection in ducts, Advanced Heat Transfer, academic Press, New York, 1978, pp. 153–195.
[23] J. Pfahler, J. Harley, H.H. Bau, J. Zemel, Liquid transport in micron and submicron channels, J. Sensors Actuators 21 (1990) 431–434.
[24] R. Bavière, F. Ayela, S. Le Person, M. Favre-Marinet, An experimental study of water flow in smooth and rough rectangular micro-channels, in: S.G. Kandlikar (Ed.), Proceedings of the Second International Conference on Microchannels and Minichannels, Rochester, June 17–19, 2004, pp. 221–228.
[25] H. Schlichting, Boundary Layer Theory, fourth ed., MacGraw & Hill, New York, 1960.
[26] J. Koo, C. Kleinstreuer, Analyses of liquid flow in microconduits, in: S.G. Kandlikar (Ed.), Proceedings of the Second International Conference on Microchannels and Minichannels, Rochester, June 17–19, 2004, pp. 191–198.
[27] P. Shen, S.K. Aliabadi, J. Abedi, A review of single-phase liquid flow and heat transfer in microchannels, in: S.G. Kandlikar (Ed.), Proceedings of the Second International Conference on Microchannels and Minichannels, Rochester, June 17–19, 2004, pp. 213–220.
[28] J.P. Holman, Heat Transfer, McGraw-Hill, New York, 1986.
[29] Z.Y. Guo, Z.X. Li, Size effect on microscale single-phase flow and heat transfer, Int. J. Heat Mass Transfer 46 (2003) 149–159.